

Robustness Analysis of Induction Generator based Variable Speed Wind Power Plant with Power Optimization Capability



Neha Gupta, Yaduvir Singh

Abstract: This paper presents power optimization of a variable speed grid connected wind power plant. We have employed a non-linear controller to improve the performance of extremum seeking (ES) scheme applied to wind power plant for power optimization. The design of the non linear controller is based on feedback linearization and feedback-oriented control idea. We have considered horizontal wind turbine functioning in sub-rated power region. The aim of this paper is to design a robust controller for power optimization, which is insensitive to the uncertainties in system parameters. The ES scheme aims at regulating the wind turbine rotor speed by changing stator electrical frequency through matrix converter. The controller designed in this work is a robust non-linear controller, which prevents magnetic saturation of induction generator and minimizes the response time of the system. The robustness of the control algorithm has been tested by adding different amount of perturbation to model's parameters. Also results with and without non linear controller have been compared.

Keywords: Wind generator, Extremum seeking, Robustness, SCIG, Controller

I. INTRODUCTION

Wind energy has proved to be an important clean, abundant and renewable source of energy [1-4]. The numerous advantages of wind turbine have motivated many engineers to build various control strategies for wind power plants, in order to optimize the performance and functioning for cost reduction. We used control theory to observe the changes in wind turbine with the variation in system parameters. The aim of this work is to design a controller for power optimization, which is insensitive to the changes in model parameters and uncertainties that may appear in the system. Since wind energy source is stochastic in nature, to keep its performance within sub-rated region, robust controller is required to perform properly in the presence of uncertainties and non-linear elements. The output power of the turbine is proportional to cube of the wind speed, the rotation speed of the turbine and the pitch angle of the blades. Here in this paper we have considered blade pitch angle to be zero [5-10].

Revised Manuscript Received on December 30, 2019.

* Correspondence Author

Neha Gupta, Pursuing Ph.D. Department of Electrical Engineering, School of Engineering, HBTU, Kanpur, Uttar Pradesh, India.

(Dr.) Yaduvir Singh, Professor & Head of Department of Electrical Engineering, School of Engineering, HBTU, Kanpur, Uttar Pradesh, India.

© The Authors. Published by Blue Eyes Intelligence Engineering and Sciences Publication (BEIESP). This is an open access article under the CC BY-NC-ND license (<http://creativecommons.org/licenses/by-nc-nd/4.0/>)

The designed controller must be able to adjust the torque of the generator in order to adapt the rotational speed of the turbine which moves the rotor. The turbines chosen for study in this paper are variable speed wind turbines and the main focus will fall on the analysis of the robustness of non-linear controller designed for such a turbine. We have also compared the robustness of system with and without inner loop control.

II. THEORITICAL BACKGROUND

A general block diagram of wind power plant contains wind turbine, WG, power electronic interface to achieve MPPT at varying wind speeds and load. Here in this paper, we are using matrix converter as power electronic interface and our wind generator is SCIG. Since we are modeling grid connected wind power plant, we have utility grid in place of load. In order to know the dynamics of wind turbine, we also need to model the wind turbine aerodynamics. The block diagram considered in this paper is shown in Fig.1.

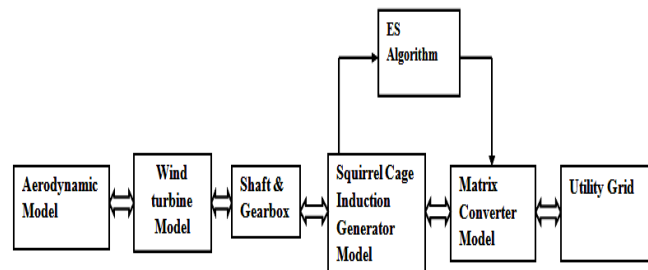


Fig.1. Block diagram of Wind power plant model under study

The power captured by the VSWT is expressed in terms power coefficient C_p , which is a dimensionless quantity. C_p is a measure of the ratio of the rotor power to the wind power:

$$P_T = \frac{1}{2} \rho A_r C_p(\lambda, \beta) V_w^3 \quad (1)$$

Maximum torque extracted from the turbine rotor can be given as

$$T_T = \frac{1}{2\omega_t} \rho A_r C_p(\lambda, \beta) V_w^3 \quad (2)$$

Where TSR (tip speed ratio) is defined as

$$\lambda = \frac{\text{blade tip speed}}{\text{wind speed}} = \frac{\omega_t \times R}{V_w}$$

V_w = speed of wind in m/s

A = swept area of wind turbine blade

ω_t = turbine angular speed.

λ = TSR and β = Pitch angle of rotor blade

C_p is related to λ , and β . Here, we have considered C_p curve to be [2]:



$$C_p = 0.73 \frac{151 \frac{V_w}{R\omega_r} - 13.635}{\exp\left(\frac{V_w}{R\omega_r} - 0.003\right)} \quad (3)$$

From Fig..2, it is clear that C_p remains at the same level, if the turbine speed is varied with each change in wind speed.

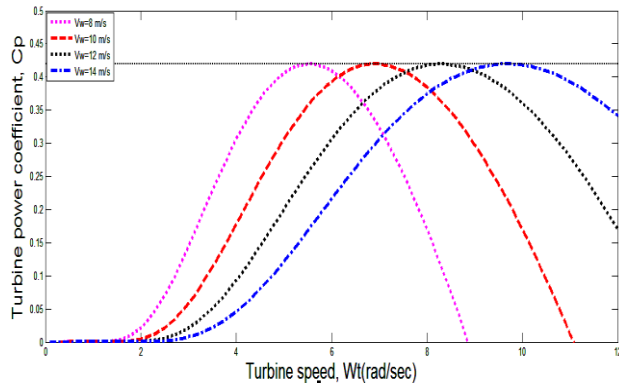


Fig..2. power coefficient vs. turbine speed curve

Fig..3 shows the change in turbine power with each change in angular velocity for different wind speeds.

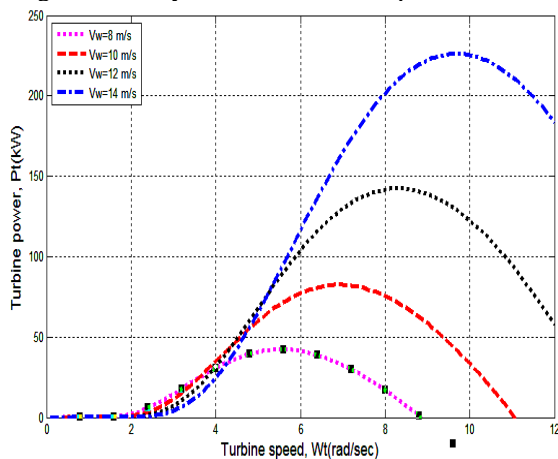


Fig..3. turbine power vs. turbine speed curve

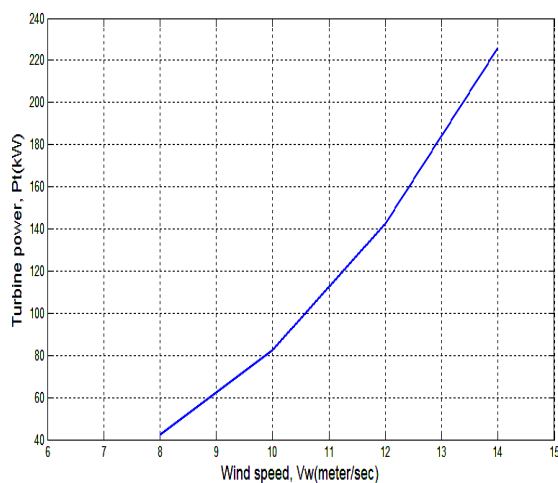


Fig..4 Turbine speed vs. wind speed curve

Fig..4. shows that if we join the points of at which the turbine power is maximum, a curve of third-order defining the maximum power attained by the wind turbine is obtained.

III. MATHEMATICAL MODEL OF WIND POWER PLANT

The overall model for wind energy conversion system may be given by following eight nonlinear equations, which includes the state-equation of the mechanical shaft, electrical generator, and the matrix converter [11-14].

$$\frac{d}{dt} i_\alpha = -a_0 i_\alpha + a_1 \lambda_\alpha + a_2 \omega_r \lambda_\beta + \frac{\cos \delta_0}{\sigma L_s} V_{0m} \quad (4)$$

$$\frac{d}{dt} i_\beta = -a_0 i_\beta + a_1 \lambda_\beta + a_1 \omega_r \lambda_\alpha + \frac{\sin \delta_0}{\sigma L_s} V_{0m} \quad (5)$$

$$\frac{d}{dt} \lambda_\alpha = a_3 i_\alpha - a_4 \lambda_\alpha - \omega_r \lambda_\beta \quad (6)$$

$$\frac{d}{dt} \lambda_\beta = a_3 i_\beta - a_4 \lambda_\beta + \omega_r \lambda_\alpha \quad (7)$$

$$\frac{d}{dt} \theta_0 = \omega_0 \quad (8)$$

$$\frac{d}{dt} \omega_r = \frac{3p^2 L_m}{2L_r J} (i_\beta \lambda_\alpha - i_\alpha \lambda_\beta) - \frac{pK_s}{n_j} \dot{\theta} - \frac{pB}{n_j} (\omega_t - \frac{\omega_r}{pn}) \quad (9)$$

$$\frac{d}{dt} \dot{\theta} = \omega_t - \frac{\omega_r}{pn} \quad (10)$$

$$\frac{d}{dt} \omega_t = -\frac{P_t(V_w \omega_t)}{J_s \omega_t} - \frac{K_s}{J_s} \dot{\theta} - \frac{B}{J_s} (\omega_t - \frac{\omega_r}{pn}) \quad (11)$$

IV. EXTREMUM SEEKING FOR MAXIMUM POWER EXTRACTION IN WIND POWER PLANT

A typical power curve of a WECS as shown in Fig..5 can be divided into four major regions. The first region contains the velocities below which turbine is not able to generate any power due to insufficient wind. The second region contains the wind velocities from where the generation starts to the velocity up till which the power linearly increases with increase in wind velocity. This region is known as sub-rated power region. This is the region where MPPT schemes are applied to capture maximum power; hence power output is limited by wind turbine. The fourth region contains the velocities of wind which are much stronger and may cause damage to wind turbine, hence in this region, the turbine is shut down [18].

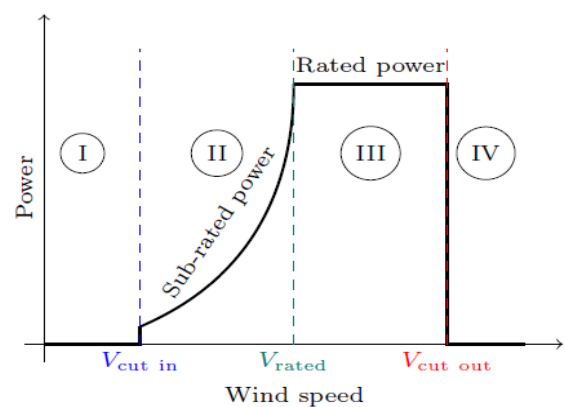


Fig..5. Wind speed vs. power curve showing four operating regions [18].

Now we present the extremum seeking technique for WECS, which is a real time optimization technique and unlike conventional MPPT algorithms it does not require system modeling and identification. For simulation purpose the models of C_p and turbine power are given eq. (3) and (4). Here it is assumed that we can measure & manipulate turbine power through MC [16]. As, the turbine power map has one MPP under any wind speed, we make the following assumption

For $V_{cut\ in} < V_w < V_{rated}$ (Fig..5).

$$\frac{\partial P_t(V_w, \omega_t)}{\partial \omega_t}(\omega_t^*) = 0 \tag{12}$$

$$\frac{\partial^2 P_t(V_w, \omega_t)}{\partial^2 \omega_t}(\omega_t^*) < 0 \tag{13}$$

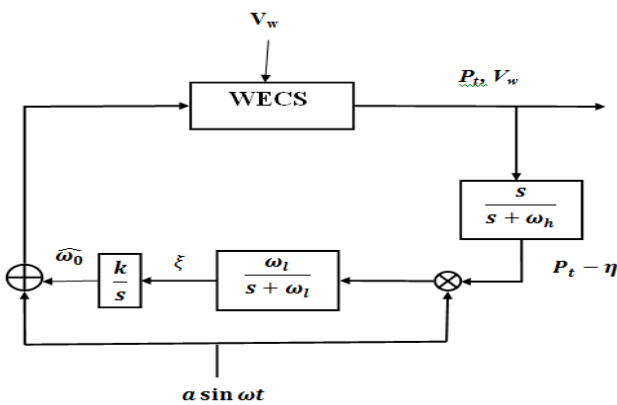


Fig.6. Extremum seeking scheme for extraction of maximum power in wind power plant (without inner loop).

If, we carefully study the torque speed characteristics of an induction machine, it is observed that this curve is very sharp near the synchronous speed (stator electrical frequency), ω_0 . At this point the rotor electrical speed ω_r and synchronous speed ω_0 will be nearly equal. This indicates that if we change the stator electrical frequency, the electrical rotor speed will change, which intern will change the turbine speed ω_t [19-20]. Thus by varying ω_0 through MC, we may change turbine speed ω_t to track MPPT. Our ES scheme works on the same line.

V. MATHEMATICAL MODEL OF PROPOSED NON LINEAR STATE FEEDBACK CONTROLLER

The results obtained by applying ES scheme for power optimization had slow response time and low efficiency. In case of flux transient, the dynamics of system are non linear and coupled [15, 17]. So, we have proposed a non-linear controller based on field-oriented control and feedback linearization to prevent magnetic saturation of induction generator and improve the performance and response time of the system [14].

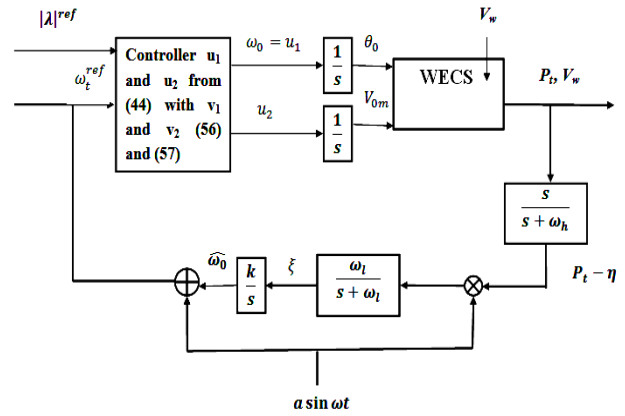


Fig. 7. Extremum seeking for MPPT in WECS with inner loop.

$$y_1 = \Psi_1(x) = x_9 \tag{14}$$

$$y_2 = \mathcal{L}_f \Psi_1(x) = -a_9 \left(x_9 - \frac{x_7}{pn} \right) - a_8 x_8 - \frac{T_t}{J} \tag{15}$$

$$y_3 = \mathcal{L}_f^2 \Psi_1(x) = b_0 \xi_q + b_1 \mathcal{L}_f \Psi_1(x) + b_2 x_8 + b_3 \frac{T_t}{J} - \frac{T_t}{J} \tag{16}$$

$$y_4 = \mathcal{L}_f^3 \Psi_1(x) = b_4 \mathcal{L}_f^2 \Psi_1(x) + b_5 \mathcal{L}_f \Psi_1(x) + b_6 x_8 - \frac{b_0}{\sigma L_s} x_6 \lambda_q - x_7 \left(b_7 \Psi_2(x) + b_8 \mathcal{L}_f \Psi_2(x) \right) + b_9 \frac{T_t}{J} + \frac{T_t}{J} - \frac{T_t}{J} \tag{17}$$

$$\eta_1 = \Psi_2(x) = x_3^2 + x_4^2 \tag{18}$$

$$\eta_2 = \mathcal{L}_f \Psi_2(x) = 2a_3 \xi_d - 2a_4 \Psi_2(x) \tag{19}$$

$$\eta_3 = \mathcal{L}_f^2 \Psi_2(x) = b_{12} \Psi_2(x) + b_{11} \mathcal{L}_f \Psi_2(x) + b_{13} x_7 \left(\mathcal{L}_f^2 \Psi_2(x) - b_1 \mathcal{L}_f \Psi_2(x) - b_2 x_8 + b_3 \frac{T_t}{J} + \frac{T_t}{J} \right) + 2a_3^2 i_s + \frac{2a_3}{\sigma L_s} x_6 \lambda_d \tag{20}$$

$$\Delta = x_8 \tag{21}$$

$$\varphi = \arctan \left(\frac{x_4}{x_3} \right) \tag{22}$$

where $\xi_d = x_1 x_3 + x_2 x_4$, $\xi_q = x_2 x_3 - x_1 x_4$, $i_s = i_\alpha^2 + i_\beta^2$

and

$$\begin{bmatrix} \lambda_d \\ \lambda_q \end{bmatrix} = \begin{bmatrix} \cos x_5 & \sin x_5 \\ -\sin x_5 & \cos x_5 \end{bmatrix} \begin{bmatrix} x_3 \\ x_4 \end{bmatrix} \tag{23}$$

The inverse transformation of (14)-(22)

$$\begin{bmatrix} x_1 \\ x_2 \end{bmatrix} = \frac{1}{\sqrt{\eta_1}} \begin{bmatrix} \cos \varphi & -\sin \varphi \\ \sin \varphi & \cos \varphi \end{bmatrix} \begin{bmatrix} \Psi_d \\ \Psi_q \end{bmatrix} \tag{24}$$

$$x_3 = \sqrt{\eta_1} \cos \varphi \tag{25}$$

$$x_4 = \sqrt{\eta_1} \sin \varphi \tag{26}$$

$$x_5 = \arctan \left(\frac{Y_\beta}{Y_\alpha} \right) \tag{27}$$

$$x_6 = \sqrt{Y_\alpha^2 + Y_\beta^2} \tag{28}$$

$$x_7 = pn \left(y_1 + \frac{y_2}{a_9} + \frac{a_3}{a_9} \Delta + \frac{T_t}{a_9 J} \right) \tag{29}$$

$$x_8 = \Delta \tag{30}$$

$$x_9 = y_1 \quad (31)$$

$$\Psi_d = \frac{\eta_2 + 2a_4\eta_1}{2a_3} \quad (32)$$

$$\Psi_q = \frac{1}{b_0} \left(y_3 - b_1 y_2 - b_2 \Delta - b_3 \frac{T_t}{J} + \frac{T_t}{J} \right) \quad (33)$$

With

$$\Phi_d = \frac{\sigma L_s}{2a_3} (\eta_2 + 2a_4\eta_1 - 2a_1 a_3 \eta_1 - 2a_3^2 i_s) \quad (34)$$

$$\Phi_q = \frac{\sigma L_s}{b_0} \left(y_4 - b_1 y_3 + \frac{a_3^2}{a_2^2} y_2 + \frac{a_3^2}{a_2^2} \Delta + b_0 (a_0 + a_4) \Psi_q + b_0 x_7 (\Psi_q + a_2 \eta_1) + \frac{a_3^2 T_t}{a_2^2 J} - b_3 \frac{T_t}{J} \right) \quad (35)$$

Assigning a new variable for each differential, we obtain:

$$\dot{y}_1 = y_2 \quad (36)$$

$$\dot{y}_2 = y_3 \quad (37)$$

$$\dot{y}_3 = y_4 \quad (38)$$

$$\dot{y}_4 = G_1 + \frac{b_0 \lambda_d}{\sigma L_s} x_6 u_1 - \frac{b_0 \lambda_q}{\sigma L_s} u_2 \quad (39)$$

$$\dot{\eta}_1 = \eta_2 \quad (40)$$

$$\dot{\eta}_2 = \eta_3 \quad (41)$$

$$\dot{\eta}_3 = G_2 + \frac{2a_3 \lambda_q}{\sigma L_s} x_6 u_1 - \frac{2a_3 \lambda_d}{\sigma L_s} u_2 \quad (42)$$

With

$$\begin{bmatrix} \dot{i}_d \\ \dot{i}_q \end{bmatrix} = \begin{bmatrix} \cos x_5 & \sin x_5 \\ -\sin x_5 & \cos x_5 \end{bmatrix} \begin{bmatrix} x_1 \\ x_2 \end{bmatrix} \quad (43)$$

Defining the signal as follows

$$\begin{bmatrix} x_6 u_1 \\ u_2 \end{bmatrix} = \frac{\sigma L_s}{\sqrt{\eta_1}} \begin{bmatrix} \cos(\varphi - \theta_0) & -\sin(\varphi - \theta_0) \\ \sin(\varphi - \theta_0) & \cos(\varphi - \theta_0) \end{bmatrix} \begin{bmatrix} v_1 - G_1 \\ v_2 - G_2 \\ 2a_3 \end{bmatrix} \quad (44)$$

Assigning new set of variables again, we get:

$$z = [y_1 - \omega_r^{ref}, y_2, y_3, y_4]^T \quad (45)$$

$$\zeta = [\eta_1 - (|\lambda|^{ref})^2, \eta_2, \eta_3]^T \quad (46)$$

We obtain

$$\dot{z}_1 = z_2 \quad (47)$$

$$\dot{z}_2 = z_3 \quad (48)$$

$$\dot{z}_3 = z_4 \quad (49)$$

$$\dot{z}_4 = v_1 \quad (50)$$

$$\dot{\zeta}_1 = \zeta_2 \quad (51)$$

$$\dot{\zeta}_2 = \zeta_3 \quad (52)$$

$$\dot{\zeta}_3 = v_2 \quad (53)$$

$$\dot{\Delta} = -\frac{z_2}{a_0} - \frac{a_3}{a_0} \Delta - \frac{T_t}{a_0 J} \quad (54)$$

$$\dot{\varphi} = \omega_r + \frac{a_3}{b_0 \eta_1} \left(z_3 - b_1 z_2 - b_2 \Delta - b_3 \frac{T_t}{J} + \frac{T_t}{J} \right) \quad (55)$$

Linear state feedback

$$v_1 = -k_1 z_1 - k_2 z_2 - k_3 z_3 - k_4 z_4 \quad (56)$$

$$v_2 = -k_1 \zeta_1 - k_2 \zeta_2 - k_3 \zeta_3 \quad (57)$$

Definitions of all the constant parameters used in the mathematical modeling are given in Table-I

VI. SIMULATION RESULTS

The proposed extremum seeking feedback scheme for MPPT in WECS has been evaluated by testing it for different disturbances i.e. variation of wind speeds in sub rated power region using MATLAB m-file code. The results are presented below. To check the performance of inner loop we applied a wind velocity of 10 m/s for 30s and then changed it suddenly to 11 m/s. Fig.8. shows the responses of the proposed WECS incorporating the ES based control of SCIG with and without inner loop control, for sudden wind speed variation. It is seen clear from Fig. 9 & 10 that without inner loop the power coefficient greatly varies with change in wind speed but with inner loop the variation of Cp with change in speed is very less, while with increase in wind speed the power level increases.

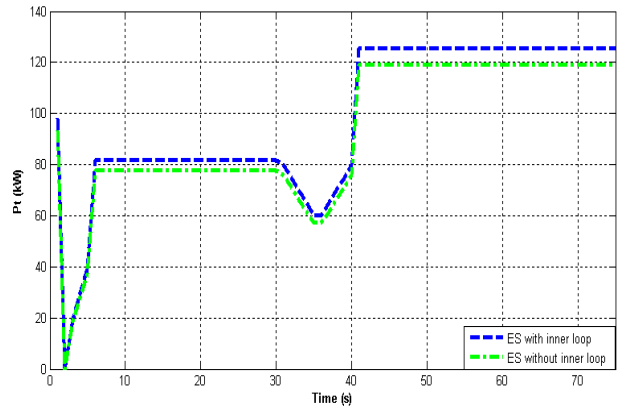


Fig.8. MPPT without inner loop, (dotted green line)MPPT with inner loop, (dotted blue line)

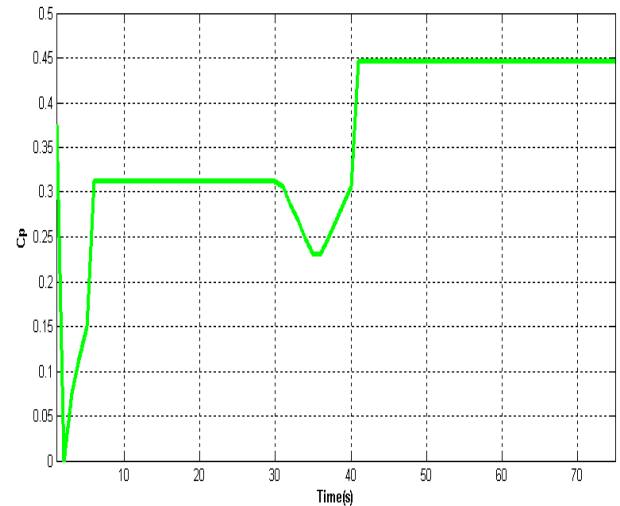


Fig.9. Power coefficient variation with inner loop control

Table- I: Constant Parameters of WECS model

a_0	$a_2 a_3 + \frac{R_s}{\sigma L_s}$	b_2	a_8^2/a_9
a_1	$a_2 a_4$	b_3	$a_8/a_9 + a_7/pn$
a_2	$\frac{L_m}{\sigma L_s L_r}$	b_4	$b_1 - a_0 - a_4$
a_3	$\frac{L_m R_r}{L_r}$	b_5	$a_0 b_1 + a_4 b_1 - b_2/a_9$
a_4	$\frac{R_r}{L_r}$	b_6	$a_0 b_2 + a_4 b_2 - a_8 b_2/a_9$
a_5	$3p^2 L_m/2JL_r$	b_7	$a_2 b_0 + a_4 b_0/a_3$
a_6	pK_s/Jn	b_8	$b_0/2a_3$
a_7	pB/Jn	b_9	$a_0 b_3 + a_4 b_3 - b_2/a_9$
a_8	$K_s/J\tau$	b_{10}	$b_3 - a_0 - a_4$
a_9	$B/J\tau$	b_{11}	$a_0 + 3a_4$
b_0	$\frac{a_5 a_9}{pn}$	b_{12}	$2a_1 a_3 - 2a_0 a_4 - 2a_4^2$
b_1	$a_8/a_9 + a_7/pn - a_9$	b_{13}	$2a_3/b_0$

VII. CONCLUSION

We have presented extremum seeking feedback algorithm for maximum power extraction in wind power plant. With our non linear controller in addition with the ES scheme we achieved more efficient results compared with ES scheme alone. We tested the performance of our proposed control system for sudden wind variation with and without the non linear controller in the inner loop and found that the system with nonlinear controller responds quicker as we change the wind velocity and hence improves the transient performance of the proposed wind power plant. While doing robustness analysis of the proposed system with and without inner loop control, we found that system with inner loop is more robust than that without inner loop control.

REFERENCES

1. Jiawei Chen, Jiechen, chunying Gong. On optimizing the transient load of variable speed wind energy conversion system during MPP tracking process. IEEE transaction on Industrial Electronics 2013; 61(9): 4698-4706.
2. S. M. Barakati. Modeling and controller design of a wind energy conversion system including a matrix converter. Ph.D., University of Waterloo, Waterloo, Canada, 2008.
3. X. She, A. Q. Huang, F. Wang, and R. Burgos. Wind energy system with integrated functions of active power transfer, reactive power compensation, and voltage conversion. IEEE Trans. Ind. Electron 2013; 60(10): 4512-4524.
4. L. Barote, C. Marinescu, and M. N. Cirstea. Control structure for single-phase stand-alone wind-based energy sources. IEEE Trans. Ind. Electron.; 60, (2): 764-772.
5. N. Wang, K. E. Johnson, and A. D. Wright. Comparison of strategies for enhancing energy capture and reducing loads using LIDAR and feed forward control. IEEE Trans. Control Syst. Technology 2013; 21(4): 1129-1142.
6. L. Shuhui, T. A. Haskew, K. A. Williams, and P. R. Swatloski. Control of DFIG wind turbines with direct-current vector control configuration. IEEE Trans. Sustain. Energy 2012; 3(1): 1-11.
7. M. F. M. Arani and E. F. El-Saadany. Implementing virtual inertia in DFIG-based wind power generation. IEEE Trans. Power Syst. 2013; 28(2): 1373-1384.
8. T. H. Nguyen and D.-C. Lee. Advanced fault ride-through technique for PMSG wind turbine systems using line-side converter as STACOM. IEEE Trans. Ind. Electron. 2013; 60(7): 2842-2850.
9. S. Zhang, K. J. Tseng, and T. D. Nguyen. Modeling of AC-AC matrix converter for wind energy conversion system. In Proc. IEEE Conf. Ind. Electron. Appl.; May 2009, pp. 184-191.
10. A. I. Bratcu, E. C. Iulian Munteanu, and S. Epure. Energetic optimization of variable speed wind energy conversion systems by extremum seeking control. In The International Conference on "Computer as a Tool; 2007.
11. P. C. Krause, O. Wasynczuk, and S. D. Sudhoff. Analysis of Electric Machinery and Drive Systems. 2nd ed. New York, NY, USA: Wiley, 2002.
12. A. D. Luca and G. Ulivi. Dynamic decoupling of voltage frequency-controlled induction motors. In Proc. 8th Int. Conf Anal. Optim. Syst.; 1988, pp. 127-137.
13. A. D. Luca and G. Ulivi. Design of exact nonlinear controller for induction motors. IEEE Trans. Autom. Control 1989; 34(12): 1304-1307.
14. R. Marino, S. Peresada, and P. Valigi. Adaptive input-output linearizing control of induction motors. IEEE Trans. Autom. Control 1993; 38(2): 208-221.
15. M. Komatsu, H. Miyamoto, H. Ohmori, and A. Sano. Output maximization control of wind turbine based on extremum control strategy. In Proc. of American Control Conference; 2001.
16. V. Kumar, R. R. Joshi, and R. C. Bansal. Optimal control of matrixconverter- based WECS for performance enhancement and efficiency optimization. IEEE Transaction on Energy Conversion 2009; 24: 264-273.

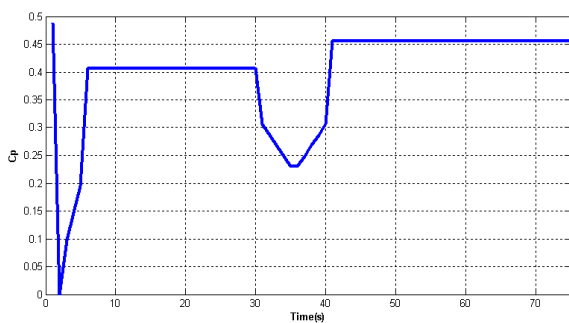


Fig..10. Power coefficient variation with inner loop control

In order to do the robustness analysis of the proposed system we have applied different perturbation to stator and rotor resistance and inductance. As it can be seen from Fig..11 that we applied an increment in rotor resistance at time 15 s then back to its previous value at 25 s similarly again increment at 50 s back to the previous value at 55 s. We observe that as the resistance is changed the power output changes for few seconds but within few seconds it recovers the required power for that corresponding wind speed. Moreover, we also observe that wind power plant with inner loop control responds faster as compared to the wind power plant without inner loop control, i.e. system is more robust with inner loop control.

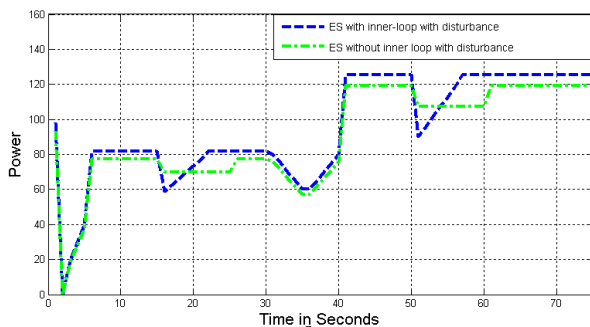


Fig. 11. Robustness analysis with an increment in the rotor

Resistor for the proposed algorithm. Variation of turbine power with inner loop (dotted blue line) with perturbation and Variation of turbine power without inner loop (dashed green line) without perturbation

Robustness Analysis of Induction Generator based Variable Speed Wind Power Plant with Power Optimization Capability

17. T. Pan, Z. Ji, and Z. Jiang. Maximum power point tracking of wind energy conversion systems based on sliding mode extremum seeking control. In Proc. IEEE Energy 2030 Conference; 2008.
18. A. Ghaffari, M. Krstic, S. Seshagiri. Power optimization and control in wind energy conversion system using extremum seeking. IEEE Transaction on Control System Technology 2014; 22(5): 1684 - 1695.
19. M. Krstić and H.-H. Wang. Stability of extremum seeking feedback for general nonlinear dynamic systems. Automatica 2000; 36(4): 595–601.
20. Khalil, H.K. Nonlinear systems. (2nd ed.). Englewood Cliffs, NJ: Prentice Hall; 1996.

AUTHORS PROFILE



Neha Gupta is presently pursuing Ph.D. Department of Electrical Engineering at School of Engineering, HBTU, Kanpur, under Prof. (Dr.) Yaduvir Singh. She has 2 research publications in SCI listed journals and 2 research papers in the conferences. She possesses nearly nine years of teaching and research experience at UG, PG and Ph.D. of engineering and technology.



Prof. (Dr.) Yaduvir Singh is presently Professor & Head of Department of Electrical Engineering at School of Engineering, HBTU, Kanpur Prof. (Dr.) Yaduvir Singh has 17 research publications in SCI listed journals and several research papers in the conferences. Prof. (Dr.) Yaduvir Singh possesses nearly twenty-seven years of teaching and research experience at UG, PG and Ph.D. of engineering and technology. He has guided more than 65 projects, 59 master level theses / dissertations and 13 PhDs.